

Impact of ultrathin transition metal buffer layers on Fe₃O₄ thin films

P. B. Jayathilaka,¹ C. A. Bauer,¹ D. V. Williams,¹ M. C. Monti,² J. T. Markert,² and Casey W. Miller^{1,a)}

¹Department of Physics, Center for Integrated Functional Materials, University of South Florida, 4202 East Fowler Avenue, Tampa, Florida 33620, USA

²Department of Physics, University of Texas at Austin, 1 University Station C1600, Austin, Texas 78712, USA

(Presented 22 January 2010; received 21 October 2009; accepted 19 November 2009; published online 19 April 2010)

3000 Å Fe₃O₄ (magnetite) thin films were simultaneously grown on (001) MgO single crystal substrates with and without 30 Å buffer layers of Fe, Cr, Mo, and Nb. For all samples, the Verwey transition temperature (T_V) occurs between 119 and 125 K, indicating good oxygen stoichiometry. We observe highly oriented (001) Fe₃O₄ with Mo and no buffer layer, reduced (001) texture with Nb and Fe, and polycrystalline growth with Cr. Mo, Cr, and unbuffered magnetite show typical magnetic behavior, whereas Nb and Fe buffers lead to anomalous magnetic properties that may be due to interfacial reactivity. © 2010 American Institute of Physics. [doi:10.1063/1.3350910]

Present interest in magnetite originates from its supposed half-metallic nature and potential utility in oxide spintronics,^{1,2} its utility in biomedical applications,^{3,4} as well as open questions about the well known Verwey transition.^{5,6} Although it is among the most widely studied magnetic materials, the growth of magnetite thin films continues to be perturbed and improved.⁷⁻¹⁴ Due to the nearly ideal lattice match, MgO (100) is typically the substrate of choice for magnetite film growth. Despite this lattice matching, however, the properties of magnetite thin films differ significantly from that of bulk magnetite. For instance, the magnetization may not be saturated even in fields as large as 70 kOe;⁷ misoriented magnetite grains have been observed near the substrate, with some persisting toward the sample surface;⁸ single crystal Fe₃O₄ on MgO (100) is under tensile stress¹⁵; antiphase boundaries, potentially related to the previous items, plague thin films.^{16,17} Buffer layers affect the magnetite growth, but not always beneficially. A Ru buffer layer on MgO (110) reduced lattice strain in the magnetite, but negative impacts on other properties were observed, most notably, a suppression of the Verwey transition.¹³ Fe and Cr buffers on MgO (100) lead to improved Fe₃O₄ squareness ratios, low saturation fields, reduced antiphase boundary density, and saturation magnetization approaching bulk values, but the impact on the Verwey transition is not clear.¹⁶ Here, we study in detail the impact of thin Fe, Cr, Mo, and Nb buffer layers on the structure and magnetism of magnetite films.

All samples were grown by dc magnetron sputtering on MgO (100) substrates in a system with a base pressure of 20 nTorr using ultrahigh purity gases. An *in situ* mask exchanging apparatus in the load lock (200 nTorr) enabled the growth of four different transition metal (TM) buffer layers on individual substrates, followed by the simultaneous deposition of Fe₃O₄ on all substrates, including one unbuffered control sample. Consequently, we can ascribe any differences in

magnetite's physical properties to the buffer layers. The 30 Å buffer layers of Nb, Mo, Cr, and Fe were deposited at 300 °C in 3 mTorr of Ar flowing at 20 SCCM (SCCM denotes standard cubic centimeter per minute). Under these conditions, 300 Å TM films are (001) oriented with good structural coherence in the growth direction and low mosaic spread (Fig. 1, inset). The deposition rates under these conditions with 100 W dc power were 0.80, 0.85, 0.68, and 0.65 Å/s, respectively, as measured by x-ray reflectivity on thicker films. After depositing all the buffers layers sequentially, the

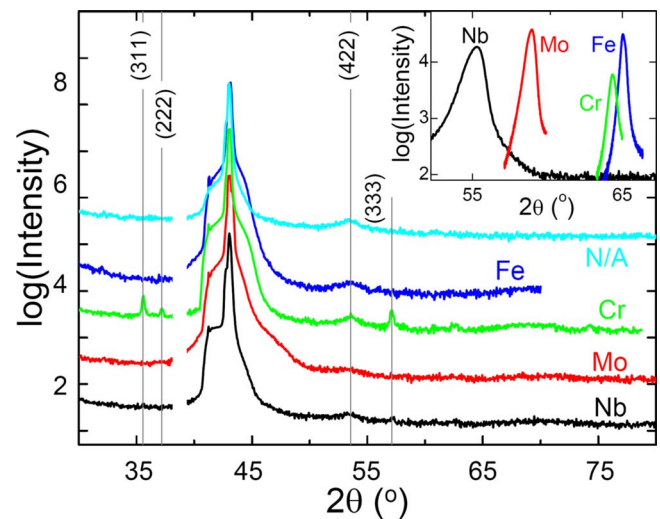


FIG. 1. (Color online) Wide angle x-ray diffraction measurements of MgO(001)/TM(30 Å)/Fe₃O₄(3000 Å)/Cr(30 Å). Each curve is labeled by its buffer layer. A Cr buffer leads to polycrystalline Fe₃O₄, with the observed orientations indicated, while the others lead to strongly (001) oriented Fe₃O₄. The main (004) Fe₃O₄ peak is likely coincident with the MgO (002) peak and is thus unobservable. The Fe₃O₄ was grown simultaneously on all samples after depositing the individual TM layers without breaking vacuum. The (422) peak is only present in samples with a Cr capping layer. (Inset) (002) peaks of 300 Å Nb, Mo, Cr, and Fe films grown on (001) MgO at 300 °C are highly (001) oriented (Ref. 18). These (002) peaks had FWHM of (Bragg, rocking): Nb (0.79°, 1.69°), Mo (0.46°, 0.63°), Cr (0.41°, 1.00°), and Fe (0.32°, 0.36°).

^{a)}Electronic mail: cmiller@cas.usf.edu.

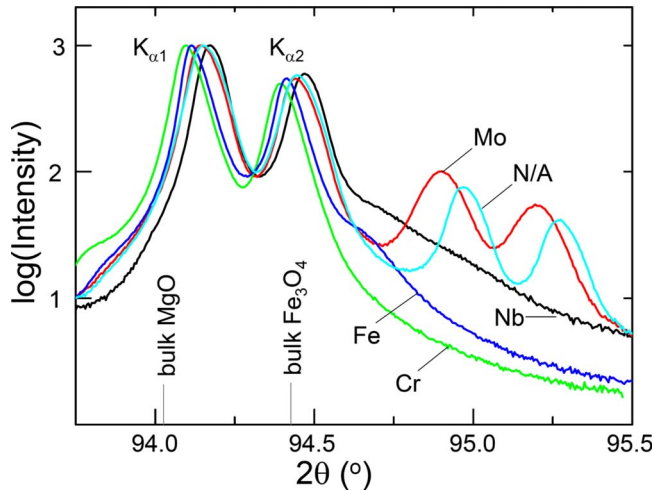


FIG. 2. (Color online) The MgO and Fe₃O₄ diffraction peaks are resolvable for higher order reflections. The MgO (004) and Fe₃O₄ (008) appear as doublets because of the two Cu $K\alpha_1$ wavelengths. Each curve is labeled by its buffer layer. The presence of Fe₃O₄ (008) peaks indicates that highly oriented magnetite was grown on Nb, Fe, Mo, and N/A buffer layers, with the latter two yielding the highest quality magnetite. The Fe₃O₄ was grown simultaneously on all samples after depositing the individual TM layers without breaking vacuum. The positions of bulk MgO and Fe₃O₄ for Cu $K\alpha$ radiation are noted for reference.

mask was removed entirely, exposing all five substrates for magnetite growth. The 3000 Å magnetite layer was grown from an Fe target by reactive sputtering at 200 W, 300 °C, in a total pressure of 10 mTorr with Ar and O₂ flow rates fixed at 20 and 0.75 SCCM, respectively. The films were capped with a 30 Å Cr layer to limit oxidation. The samples were rotated at 40 rpm during growth to obtain uniform film thicknesses.

Figure 1 shows x-ray diffraction scans of four buffer layer samples MgO(001)/TM(30 Å)/Fe₃O₄(3000 Å)/Cr(30 Å), where TM=Nb, Mo, Cr, and Fe, and one with no buffer (denoted N/A). The only diffraction peaks observed are from magnetite and the substrate. The low intensity (422) peak apparent in all five samples does not exist in uncapped samples, suggesting that the Cr cap influences the top of the magnetite. Aside from this, only the Cr buffered sample exhibits multiple Fe₃O₄ orientations. MgO and Fe₃O₄ have very little lattice mismatch, which causes the intense (002) MgO peak to drown out the (004) magnetite peak. However, it is possible to resolve the two materials by inspecting higher order peaks. The existence of the (008) peaks shown in Fig. 2 indicates that each of the Fe₃O₄ samples has (001) texture except Cr, which shows no observable (008) peak. Based on their (008) intensities, Mo and N/A buffers lead to Fe₃O₄ with the greatest (001) texture. Rocking curves of these samples have FWHM of 0.055° and 0.079°, respectively, implying low mosaic spread. Comparison with the MgO (004) peaks notes that these peaks are instrumentally broadened, further underscoring their structural quality. The Fe₃O₄ (008) peaks from the Nb buffered sample are low intensity, but clearly observable. Only one Fe₃O₄ (008) peak is observed for the Fe buffered sample, implying that the $K\alpha_1$ peak is likely coincident with the MgO (004) $K\alpha_2$ peak. This suggests that the Fe/Fe₃O₄ sample is nearly strain-free

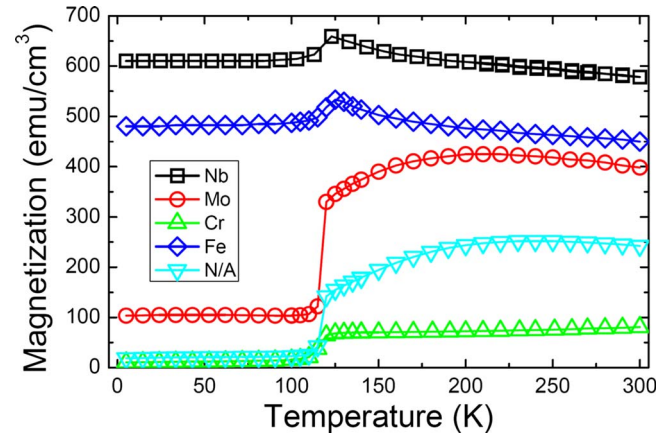


FIG. 3. (Color online) The Verwey transition occurs between 119 and 125 K, indicating good oxygen stoichiometry. The Fe and Nb buffered samples show anomalous responses, whereas the Mo, Cr, and unbuffered samples have responses similar to bulk behavior. The magnetite was grown simultaneously on all samples.

relative to bulk magnetite ($d_{\text{bulk}}=8.3967$ Å). This may be related to the reduced density of antiphase boundaries previously noted of Fe buffered samples.¹⁶ Nb, Mo, and N/A buffers also lead to small strain parameters: -0.26% , -0.38% , and -0.44% , respectively. While the films are slightly strained relative to the bulk, the fact that the (008) peaks are instrumentally broadened for Mo and N/A samples suggests that the d-spacing in the momentum transfer direction is uniform throughout the film's thickness. It is difficult to conclude the same for the Nb and Fe samples.

Superconducting quantum interference device magnetometry was used for zero-field-cooled measurements of the magnetization along the (100) direction in a field of 100 Oe after saturating the samples to 30 kOe at 300 K. Hysteresis loops were subsequently measured at various temperatures out to fields of ± 5 kOe.

Figure 3 shows the temperature dependent magnetization of the samples. The Mo, Cr, and unbuffered samples show characteristic magnetite behavior, with an abrupt change in magnetization at the Verwey transition temperature, T_V . The Nb and Fe buffered samples, however, show an anomalous peak in magnetization near T_V , and have low temperature magnetization substantially exceeding that of bulk magnetite. The observed transition temperatures indicate good oxygen stoichiometry.¹⁹

As with the M - T data, the samples show two types of hysteresis behavior. Figure 4 shows hysteresis loops of Mo (similar to Cr and unbuffered) and Nb (similar to Fe) buffered samples above and below T_V . Both samples show increased coercivity when cooled below T_V , with the Mo changing more dramatically. Defining the loop squareness as $1 - M_r / (\chi_c H_c)$, where M_r is the remanent magnetization and χ_c is dM/dH at the coercive field, H_c , we note that the Mo sample shows a decrease in squareness, while the Nb sample has nearly constant squareness.

The anomalous behavior of the Nb and Fe buffer layers may be related to their relatively high reactivity. Some possibilities include Nb/Fe becoming oxidized themselves during the initial stages of reactive sputtering, which could lead

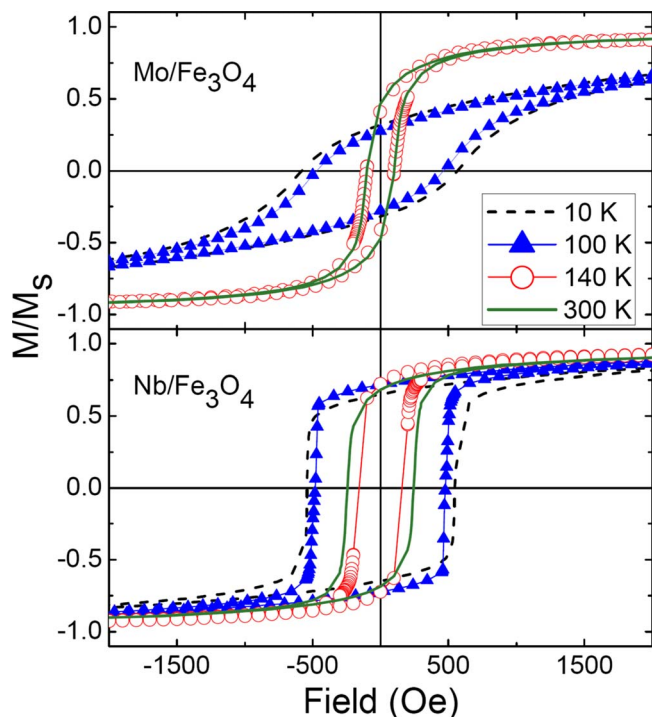


FIG. 4. (Color online) M - H above and below T_V for Mo and Nb buffered magnetite samples. The diamagnetic background signal has been subtracted. The legend applies to both panels.

to significant strain and nonideal buffer layer; Nb/Fe reducing the magnetite, resulting in an interface stoichiometry of the sort $(\text{Nb or Fe})\text{O}_x\text{-FeO}_x$. That the nonmagnetic Nb buffered sample shows larger magnetization than the Fe buffered sample suggests that it is unlikely that the former would lead to anomalous magnetic properties of the magnetite. The latter, however, could result in an internal coupling between the proposed interfacial oxide and the “bulk” of the magnetite film; the temperature dependence of the bulk may lead to a temperature dependent competition that governs the total magnetization.^{20,21}

In conclusion, we have demonstrated that ultrathin TM buffer layers can significantly impact the structure and magnetism of magnetite thin films. The key to this work is that the magnetite layers were grown simultaneously on all five substrates, allowing us to make conclusions based solely on the buffer layer material. Surprisingly, the Mo, Cr, and unbuffered samples all showed similar behavior, despite the

fact that the Cr buffered magnetite appears polycrystalline. In contrast, the Nb and Fe buffered samples showed strong (001) texture but have anomalous magnetic properties. Noting that Nb and Fe are more reactive than Mo and Cr, a potential origin of these observations is that Nb and Fe may have reduced the magnetite, creating a stoichiometrically inhomogeneous material near the lower interface.

This work was supported by Grant No. NSF-ECCS 0820880 (USF), Grant No. NSF-DMR 0605828 (UT), and The Welch Foundation F-1191 (UT). D.V.W. acknowledges support from the NSF Florida Georgia Louis Stokes Alliance for Minority Participation (FGLSAMP) Bridge to the Doctorate award to USF-HRD Grant No. 0217675.

- ¹M. Bibes and A. Barthélémy, *IEEE Trans. Electron Devices* **54**, 1003 (2007).
- ²Y. S. Dedkov, U. Rüdiger, and G. Güntherodt, *Phys. Rev. B* **65**, 064417 (2002).
- ³A. Ito, M. Shinkai, H. Honda, and T. Kobayashi, *J. Biosci. Bioeng.* **100**, 1 (2005).
- ⁴J. Gass, P. Poddar, J. Almand, S. Srinath, and H. Srikanth, *Adv. Funct. Mater.* **16**, 71 (2006).
- ⁵J. García and G. Subias, *J. Phys.: Condens. Matter* **16**, R145 (2004).
- ⁶F. Walz, *J. Phys.: Condens. Matter* **14**, 203 (2002).
- ⁷D. T. Margulies, F. T. Parker, and A. E. Berkowitz, *J. Appl. Phys.* **75**, 6097 (1994).
- ⁸A. Koblishka-Veneva, M. R. Koblishka, F. Mücklich, and U. Hartmann, *Phys. Status Solidi. A* **205**, 1835 (2008).
- ⁹N.-T. Kim-Ngan, A. Balogh, J. Meyer, J. Brötz, S. Hummelt, M. Zajac, T. Slezak, and J. Korecki, *Surf. Sci.* **602**, 2358 (2008).
- ¹⁰T. Fujii, M. Takano, R. Katano, Y. Bando, and Y. Iozumi, *J. Appl. Phys.* **68**, 1735 (1990).
- ¹¹F. Schedin, L. Hewitt, P. Morrall, V. N. Petrov, G. Thornton, S. Case, M. F. Thomas, and V. M. Uzdin, *Phys. Rev. B* **58**, R11861 (1998).
- ¹²G. E. Sterbinsky, J. Cheng, P. T. Chiu, B. W. Wessels, and D. J. Keavney, *J. Vac. Sci. Technol. B* **25**, 1389 (2007).
- ¹³K. Aoshima and S. X. Wang, *J. Appl. Phys.* **91**, 7146 (2002).
- ¹⁴G. Q. Gong, A. Gupta, G. Xiao, W. Qian, and V. P. Dravid, *Phys. Rev. B* **56**, 5096 (1997).
- ¹⁵Y. Z. Chen, J. R. Sun, Y. N. Han, X. Y. Xie, J. Shen, C. B. Rong, S. L. He, and B. G. Shen, *J. Appl. Phys.* **103**, 07D703 (2008).
- ¹⁶C. Magen, E. Snoeck, U. Lüders, and J. F. Bobo, *J. Appl. Phys.* **104**, 013913 (2008).
- ¹⁷D. T. Margulies, F. T. Parker, M. L. Rudee, F. E. Spada, J. N. Chapman, P. R. Aitchison, and A. E. Berkowitz, *Phys. Rev. Lett.* **79**, 5162 (1997).
- ¹⁸J. E. Mattson, E. E. Fullerton, C. H. Sowers, and S. D. Bader, *J. Vac. Sci. Technol. A* **13**, 276 (1995).
- ¹⁹J. P. Shepherd, J. W. Koenitzer, R. Aragón, J. Spal/ek, and J. M. Honig, *Phys. Rev. B* **43**, 8461 (1991).
- ²⁰Z.-P. Li, J. Müller, W. Casey, and I. K. Schuller, *Phys. Rev. Lett.* **96**, 137201 (2006).
- ²¹F. I. F. Nascimento, A. L. Dantas, L. L. Oliveira, V. D. Mello, R. E. Camley, and A. S. Carriço, *Phys. Rev. B* **80**, 144407 (2009).